Available online at www.sciencedirect.com
SCIENCE DIRECT
ELSEVIER
Journal of Luminescence 110 (2004) 181–184
JOURNAL OF LUMINESCENCE
www.elsevier.com/locate/jlumin

Quantum interference at corners

G. Juzeliūnas[a,*], M. Al-Amri[b,c], S.C. Skipsey[b], M. Babiker[b]

[a] Vilnius University Research Institute of Theoretical Physics and Astronomy, A. Goštauto 12, 2600 Vilnius, Lithuania
[b] Department of Physics, University of York, Heslington, York YO10 5DD, UK
[c] Department of Physics, King Khalid University, Abha, Saudi Arabia

Abstract

We show that a radiating atom, or molecule, localised at sub-wavelength distances from a corner arising from the intersection of three planar material surfaces, exhibits novel quantum interference effects. The simplest case arises for a corner formed by the intersection of three perfect conductors, all at right angles. This situation is shown here to give rise to super-radiance and sub-radiance effects that are highly sensitive to the dipole moment orientation and position of the radiating atom or molecule in the vicinity of the corner.

PACS: 42.50.Ct; 34.50.Dy; 32.80.−t; 41.20.Jb

Keywords: Quantum interference; Cavity QED; Quantum information processing; Spontaneous emission

Recent years have seen remarkable developments, firstly in the ability to create material structures of almost any desired shape and composition by means of modern deposition techniques and lithography at the micrometer scale and below. Secondly, there have been impressive developments in the ability to perform delicate experiments in which the positions of single atoms and molecular centres can now be detected with nanometre accuracy [1].

Furthermore, the physics of quantum systems in a restricted space has acquired a new significance recently with the advent of investigations concerned with quantum information processing [2]. Recent experiments by Grangier and co-workers [3] employed a nitrogen colour centre in a diamond nano-crystal to perform the first quantum cryptography experiment with a single-photon source. Zoller and co-workers [4], on the other hand, envisage dipole–dipole interactions between quantum systems as the essential interaction for the realisation of two-bit quantum gate—an important element in a quantum computing architecture. However, in the sub-wavelength scale, quantum systems can be sufficiently close

*Corresponding author. Tel.: +370-5-2620945; fax: +370-5-2125361.
E-mail address: gj@itpa.lt (G. Juzeliūnas).

0022-2313/$ - see front matter
doi:10.1016/j.jlumin.2004.08.006

to material boundaries to be significantly influenced by the spatial restrictions they impose. Recent theoretical work has explored the influence of the proximity of quantum systems to a single planar surface and a thin film. The effects on level widths and shifts, as well as pair correlation phenomena have been clarified [5].

In this article, we put forward and explore a significant variant of the geometry involving material interfaces which, remarkably, has not been focused on before. The structure in question is one in which the main feature is a corner due to the intersection of three materials. The fact that such a structure can be formed from arbitrary material combinations and with their surfaces intersecting at an arbitrary angle, provides for a greater generality. For clarity, we focus here on a case in which the physics is particularly transparent, namely a corner formed due to a right angle intersection of three perfect conductors. Quantum systems localised within sub-wavelength distances from the corner experience effects that, to the best of our knowledge, are novel and could be exploited in the design of scalable architectures for quantum information processing.

Consider three planar surfaces of perfect conductors, xy, yz and xz intersecting at right angles to form a corner at $x=y=z=0$, as shown schematically in Fig. 1. The rate of spontaneous emission by an atom positioned at the point $\mathbf{r}_0 = (x_0, y_0, z_0)$ in the vicinity of the corner is generally given by

$$\Gamma(\mathbf{r}_0) = \frac{2\pi}{\hbar^2 \varepsilon_0^2} \sum_\beta |\boldsymbol{\mu}.\langle 0|\mathbf{D}(\mathbf{r}_0)|\beta\rangle|^2 \delta(\omega_0 - \omega_\beta), \quad (1)$$

where $\boldsymbol{\mu}$ is the transition dipole moment vector of the emitter, ω_0 is the emission frequency and $\mathbf{D}(\mathbf{r})$ is the operator for the transverse electric displacement field. The state-vector $|0\rangle$ represents the photon vacuum and $|\beta\rangle$ belongs to a set of *one-photon* states obeying the boundary condition at the conducting boundary S:

$$\langle 0|\boldsymbol{\tau}.\mathbf{D}(\mathbf{r})|\beta\rangle = 0 \quad (2)$$

for $\mathbf{r} \in S$, where $\boldsymbol{\tau} \equiv \boldsymbol{\tau}(\mathbf{r})$ is a vector tangential to the surface S. Using the identity $\delta(\omega_0 - \omega_\beta) = \pi^{-1}\mathrm{Im}(\omega_0 - \omega_\beta - \mathrm{i}\eta)^{-1}$, with $\eta \longrightarrow 0+$, the emission rate in Eq. (1) can be rewritten as

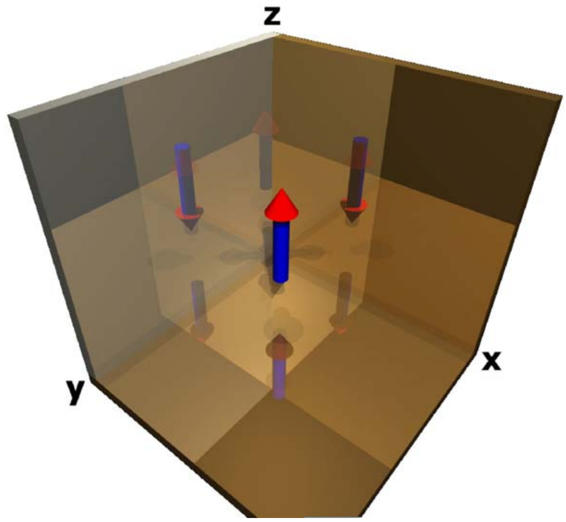

Fig. 1. Schematic arrangement of the region of space containing the corner created by three perfectly conducting planes yz and xz and xy intersecting at right angles. The emitter dipole moment vector is shown here pointing in the z-direction.

$$\Gamma(\mathbf{r}_0) = \mathrm{Im}\{\boldsymbol{\mu}^* \overset{\leftrightarrow}{\boldsymbol{\Theta}}(\mathbf{r}_0)\boldsymbol{\mu}\}, \quad (3)$$

where the tensor

$$\overset{\leftrightarrow}{\boldsymbol{\Theta}}(\mathbf{r}_0) = \frac{2}{\hbar^2 \varepsilon_0^2} \left\langle 0 \middle| \mathbf{D}(\mathbf{r}_0) \left\{ \omega_0 - \frac{H_{\mathrm{rad}}}{\hbar} - \mathrm{i}\eta \right\}^{-1} \times P_S \mathbf{D}(\mathbf{r}_0) \middle| 0 \right\rangle \quad (4)$$

describes the quantised electromagnetic field in the presence of the edge. Here H_{rad} is the Hamiltonian of the free radiation field, and $P_S = \sum_\beta |\beta\rangle\langle\beta|$ is a unit projection operator mapping the entire space of one-photon states onto the subspace obeying Eq. (2). The operator P_S takes care of the boundary condition in Eq. (4). Once the form of the projection operator P_S has been determined, one can evaluate the emission rate $\Gamma(\mathbf{r}_0)$ without expanding the electric displacement field operator $\mathbf{D}(\mathbf{r}_0)$ in terms of appropriate normal modes.

Our primary task is thus to find the correct projection operator P_S for the three orthogonal planar conducting surfaces yz, xz and xy. The first plane (to be denoted $S_\mathbf{x}$) is orthogonal to the

x-axis, the second one ($S_\mathbf{y}$) is orthogonal to the y-axis and the third one ($S_\mathbf{z}$) is orthogonal to the z-axis. We refer to these generically as $S_\mathbf{n}$ (where $\mathbf{n} = \mathbf{x}, \mathbf{y}, \mathbf{z}$), and we shall determine first the single-plane projection operator $P_\mathbf{n}$.

The one-photon states obeying the boundary condition Eq. (2) at a plane $S_\mathbf{n}$ are given by: $|\beta_\mathbf{n}\rangle \equiv |\mathbf{k}, \lambda, \mathbf{n}\rangle = |\mathbf{k}, \mathbf{e}_{\mathbf{k},\lambda,\mathbf{n}}\rangle + |-\overleftrightarrow{\mathbf{n}}\,\mathbf{k}, \overleftrightarrow{\mathbf{n}}\,\mathbf{e}_{\mathbf{k},\lambda,\mathbf{n}}\rangle$, where the tensor $\overleftrightarrow{\mathbf{n}} = 2\hat{\mathbf{n}}\hat{\mathbf{n}} - \overleftrightarrow{\mathrm{I}}$ when acting on a 3-d vector, performs a reflection of that vector in the plane $S_\mathbf{n}$, $\overleftrightarrow{\mathrm{I}}$ is a unit second rank (3×3) tensor and carets denote unit vectors. The ket $|\mathbf{k}, \mathbf{e}_{\mathbf{k},\lambda,\mathbf{n}}\rangle$ represents a plane-wave one-photon state characterised by a wave vector $\mathbf{k}$ and a polarisation unit vector $\mathbf{e}_{\mathbf{k},\lambda,\mathbf{n}}$ (with $\lambda = 1, 2$). The unit vectors $\mathbf{e}_{\mathbf{k},\lambda,\mathbf{n}}$ are chosen such that the boundary condition, Eq. (2), is satisfied at the plane $S_\mathbf{n}$. A single-plane projection operator $P_\mathbf{n}$ is then given by

$$P_\mathbf{n} = \frac{1}{2}\sum_{\mathbf{k},\lambda} |\mathbf{k}, \lambda, \mathbf{n}\rangle\langle \mathbf{k}, \lambda, \mathbf{n}| \equiv \mathrm{I} - \sum_{\mathbf{k},\lambda} |-\overleftrightarrow{\mathbf{n}}\,\mathbf{k}, \overleftrightarrow{\mathbf{n}}\,\mathbf{e}_{\mathbf{k},\lambda,\mathbf{n}}\rangle\langle \mathbf{k}, \mathbf{e}_{\mathbf{k},\lambda,\mathbf{n}}|, \tag{5}$$

where the factor $\frac{1}{2}$ prevents from the double counting. The full projection operator P_S is the product of three one-plane projection operators: $P_S = P_\mathbf{x} P_\mathbf{y} P_\mathbf{z}$, so the tensor $\overleftrightarrow{\boldsymbol{\Theta}}$ can be written as the sum of eight terms. Hence one arrives at the following decay rate:

$$\Gamma = \Gamma_{\mathrm{vac}} + \Gamma_{\mathbf{x}_0} + \Gamma_{\mathbf{y}_0} + \Gamma_{\mathbf{z}_0} + \Gamma_{\mathbf{x}_0\mathbf{y}_0} + \Gamma_{\mathbf{x}_0\mathbf{z}_0} + \Gamma_{\mathbf{y}_0\mathbf{z}_0} + \Gamma_{\mathbf{x}_0\mathbf{y}_0\mathbf{z}_0}. \tag{6}$$

The first term in Eq. (6) represents the emission rate in vacuum, namely $\Gamma_{\mathrm{vac}} = \mu^2 k_0^3 / 3\pi\varepsilon_0\hbar$, with $\mu^2 = |\mu|^2$ and $k_0 = \omega_0/c$. The remaining terms are due to the quantum interference introduced by the presence of the conductors:

$$\Gamma_{\mathbf{u}_0} = \mathrm{Im}[\overleftrightarrow{\mathbf{u}}\,\boldsymbol{\mu}\,\overleftrightarrow{\boldsymbol{\Theta}}(2\mathbf{u}_0)\boldsymbol{\mu}], \tag{7}$$

$$\Gamma_{\mathbf{u}_0\mathbf{v}_0} = \mathrm{Im}[\overleftrightarrow{\mathbf{u}}\,\overleftrightarrow{\mathbf{v}}\,\boldsymbol{\mu}^*\,\overleftrightarrow{\boldsymbol{\Theta}}(2\mathbf{u}_0 + 2\mathbf{v}_0)\boldsymbol{\mu}], \tag{8}$$

$$\Gamma_{\mathbf{x}_0\mathbf{y}_0\mathbf{z}_0} = \mathrm{Im}[\boldsymbol{\mu}^*\,\overleftrightarrow{\boldsymbol{\Theta}}(2\mathbf{x}_0 + 2\mathbf{y}_0 + 2\mathbf{z}_0)\boldsymbol{\mu}], \tag{9}$$

($\mathbf{u}$ and $\mathbf{v}$ are $\mathbf{x}$, $\mathbf{y}$ or $\mathbf{z}$, such that $\overleftrightarrow{\mathbf{u}}$ and $\overleftrightarrow{\mathbf{v}}$ become the reflection operators in the x, y or z planes, and $\mathbf{u}_0$, $\mathbf{v}_0$ become $\mathbf{x}_0$, $\mathbf{y}_0$ or $\mathbf{z}_0$), where

$$\mathrm{Im}\{\boldsymbol{\mu}_\mathbf{R}^*\,\overleftrightarrow{\boldsymbol{\Theta}}(\mathbf{R})\boldsymbol{\mu}\} = \frac{3}{2}\Gamma_{\mathrm{vac}}\left\{\xi_1\,\frac{\sin(k_0R)}{k_0R} + \xi_3\left[\frac{\cos(k_0R)}{k_0^2R^2} - \frac{\sin(k_0R)}{k_0^3R^3}\right]\right\} \tag{10}$$

is the imaginary part of the retarded dielectric tensor. The dipole orientation factors $\xi_p \equiv \xi_p(\mathbf{R})$ in Eq. (10) are defined by

$$\xi_p = \hat{\boldsymbol{\mu}}_\mathbf{R}^*.\hat{\boldsymbol{\mu}} - p(\hat{\boldsymbol{\mu}}_\mathbf{R}^*.\hat{\mathbf{R}})(\hat{\mathbf{R}}.\hat{\boldsymbol{\mu}}) \quad (p = 1, 3) \tag{11}$$

with $\boldsymbol{\mu}_{2\mathbf{u}_0} = \overleftrightarrow{\mathbf{u}}\,\boldsymbol{\mu}$; $\boldsymbol{\mu}_{2\mathbf{u}_0+2\mathbf{v}_0} = \overleftrightarrow{\mathbf{u}}\,\overleftrightarrow{\mathbf{v}}\,\boldsymbol{\mu}$ and $\boldsymbol{\mu}_{2\mathbf{x}_0+2\mathbf{y}_0+2\mathbf{z}_0} = \overleftrightarrow{\mathbf{x}}\,\overleftrightarrow{\mathbf{y}}\,\overleftrightarrow{\mathbf{z}}\,\boldsymbol{\mu}$.

The results given by Eqs. (6)–(11) can be interpreted in terms of quantum interference between the dipole emitter and its seven images in three conducting planes. The seven images consist of a set of three first-order images, positioned at $\overleftrightarrow{\mathbf{x}}\,\mathbf{r}_0 \equiv -(-x_0, y_0, z_0)$, $\overleftrightarrow{\mathbf{y}}\,\mathbf{r}_0 \equiv -(x_0, -y_0, z_0)$, and $\overleftrightarrow{\mathbf{z}}\,\mathbf{r}_0 \equiv -(x_0, y_0, -z_0)$; a second set of three second-order images, positioned at $\overleftrightarrow{\mathbf{x}}\,\overleftrightarrow{\mathbf{y}}\,\mathbf{r}_0 \equiv -(-x_0, -y_0, z_0)$, $\overleftrightarrow{\mathbf{y}}\,\overleftrightarrow{\mathbf{z}}\,\mathbf{r}_0 \equiv (x_0, -y_0, -z_0)$, and $\overleftrightarrow{\mathbf{x}}\,\overleftrightarrow{\mathbf{z}}\,\mathbf{r}_0 \equiv (-x_0, y_0, -z_0)$; and, finally, a single third-order image positioned at $\overleftrightarrow{\mathbf{x}}\,\overleftrightarrow{\mathbf{y}}\,\overleftrightarrow{\mathbf{z}}\,\mathbf{r}_0 \equiv -(-x_0, -y_0, -z_0)$. The distances between the dipolar emitter and these images are $2x_0$, $2y_0$, $2z_0$, $2|\mathbf{x}_0 + \mathbf{y}_0|$, $2|\mathbf{y}_0 + \mathbf{z}_0|$, $2|\mathbf{x}_0 + \mathbf{z}_0|$, and $2|\mathbf{x}_0 + \mathbf{y}_0 + \mathbf{z}_0|$, respectively.

Fig. 2 displays the spatial distribution of the emission rate when the dipole moment vector of the emitter near the corner is oriented along the z-axis: $\boldsymbol{\mu} = (0, 0, \boldsymbol{\mu})$. This figure is a set of brightness coded contour plots presenting the variation of $\Gamma/\Gamma_{\mathrm{vac}}$ at emitter positions (x_0, y_0, z_0), where z_0 is the value of z defining the plane. The planes are separated by distance of $\lambda/4\pi$, with λ the dipole transition wavelength. Within a given plane $z = z_0$, the rate is seen to be strongly suppressed near the $x = 0$ and $y = 0$ planes (represented by the darkest grey regions) and there are regions of super-radiance (represented by the lighter grey regions). The top plane is at $z_0 = 3\lambda/4\pi$. An emitter situated on this plane is essentially far from the corner and

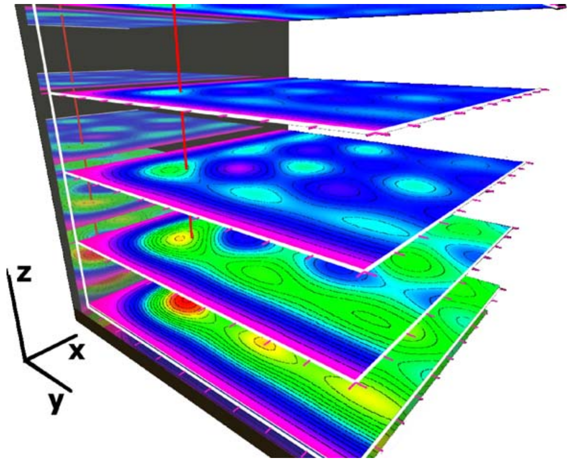

Fig. 2. Brightness coded spatial distributions of the relative emission rate $\Gamma/\Gamma_{\mathrm{vac}}$ when the emitter dipole moment vector is parallel to the z-axis, $\boldsymbol{\mu} = (0, 0, \mu)$. This figure consists of a set of a contour plots, each plot showing the variation of the relative emission rate on a plane defined by a certain value of $z_0 = 0, \lambda/4\pi, \lambda/2\pi, 3\lambda/4\pi$. The white regions represent highest values and darkest grey regions lowest values of the relative emission rate. The tick marks on the plane edges are spaced at units of $\lambda/2\pi$.

can be regarded as being near an edge, formed from two orthogonally perfect conductors. It can be shown that for small distances from the edge, satisfying $kx_0 \ll 1$ and $ky_0 \ll 1$, we have

$$\frac{\Gamma}{\Gamma_{\mathrm{vac}}} \approx \frac{1}{10} k^4 x_0^2 y_0^2. \tag{12}$$

We also note that within this plane the emitters positioned on the symmetry line $x = y$, experience the highest maxima and the lowest minima of the emission rate for that plane. The analysis of the asymptotic behaviour for small x, y as well as z_0, i.e. for dipoles close to the corner, is too involved to be presented here. This, together with details of analysis for a general dipole orientation will be presented elsewhere.

In conclusion, we have considered quantum interference effects for a quantum system situated near a corner arising from the right angle intersection of three perfect conductors. Our analysis shows that there are distinct regions where the emitter is positioned, displaying suppression and enhancement of the emission process. This property is envisaged to depend on the dipole orientation (beyond the trivial orientation alignments with the coordinate axes), an investigation now in progress. Our predictions should be experimentally verifiable for transitions in the optical region of the spectrum. At first, as proof of principle, an experiment could be conducted in the microwave region of the spectrum using a radiowave antenna as the dipolar emitter and large aluminium sheets for the material planes, along the lines of the experiment between parallel plates [6].

We suggest that this situation could be exploited as a basis for the design of a scalable architecture for quantum information processing. Suitable emitters, such as atoms, molecules, or quantum dots, could be positioned at well-defined distances in the vicinity of the edge and the direction of their dipole moment vectors can be optically controlled. Our results suggest that the emission could be switched on and off, simply by a change of the dipole orientation. In the present situation, the emission process arises as a transition from a definite entangled symmetric excited state of the emitter and its images. For two identical emitters near the corner, the expected two-body entanglement should be modified significantly by the quantum interference when the emitters are situated near the corner. The two-body entanglement need not be for emitters on a single plane parallel to one of the conductors, but the emitters could be on different planes and their dipole moment vectors could be oriented in arbitrary directions. Work on this relatively more complicated situation is now in progress.

References

[1] J. Michaelis, C. Hettich, J. Mlynek, V. Sandoghdar, Nature 405 (2000) 325.
[2] H. Lo, S. Popescu, T. Spiller, Quantum Computation and Information, World Scientific, Singapore, 1998.
[3] A. Beveratos, R. Brouri, T. Gacoin, J.P. Poizat, P. Grangier, Phys. Rev. A 64 (2001) 061802(R).
[4] D. Jaksh, J.I. Cirac, P. Zoller, S.L. Rolston, R. Cote, M.D. Lukin, Phys. Rev. Lett. 85 (2000) 2208.
[5] M. Al-Amri, M. Babiker, Phys. Rev. A 67 (2003) 438201.
[6] F.B. Seeley, J.E. Alexander, R.W. Connaster, J.S. Conway, J.P. Dowling, Am. J. Phys. 61 (1993) 545.